2003

Exfoliated Poly(Methyl Methacrylate) and Polystyrene/ Nanocomposites Occur when the Clay Cation Contains a Vinyl Monomer

Shengpei Su
Marquette University

Charles A. Wilkie
Marquette University, charles.wilkie@marquette.edu

Journal of Polymer Science Part A: Polymer Chemistry, Vol. 41, No. 8 (2003): 1124-1135. DOI.

Exfoliated Poly(Methyl Methacrylate) And Polystyrene Nanocomposites Occur When The Clay Cation Contains A Vinyl Monomer

Shengpei Su
Department of Chemistry, Marquette University, Milwaukee, WI
Charles A. Wilkie
Department of Chemistry, Marquette University, Milwaukee, WI

Abstract

The bulk polymerization of methyl methacrylate and styrene in the presence of an organically modified clay containing a vinyl group that can be involved in the polymerization produces exfoliated nanocomposites. These nanocomposites have been characterized by X-ray diffraction, transmission electron microscopy, thermogravimetric analysis, mechanical properties, and cone calorimetry. The onset temperature of thermal

degradation increases with the mechanical properties. The peak heat release rate is significantly reduced for nanocomposites containing 3 or 5% clay.

INTRODUCTION

Clay nanocomposites have been studied extensively for several years, and it is now known that most properties may be enhanced by the presence of a small amount of clay.[1] The advantages of nanocomposites are shown by the example of a 5% polyamide-6/clay nanocomposite, in which a 40% increase in the tensile strength, a 68% increase in the tensile modulus, a 60% increase in the flexural strength, and a 126% increase in the flexural modulus, along with an increase in the heat distortion temperature from 65 to 152 °C and a decrease in the impact strength by only 10%, can be observed.[2]

The compatibility between the polymer and the clay is crucial for the formation of well-dispersed nanocomposites. As the natural clay is a highly polar, inorganic material, it is important to improve its organophilicity to be compatible with the organic polymer. The modification of the clay has been accomplished by changes in the gallery space of the clay by ion exchange or cation complexation to increase the *d*-spacing and hydrophobic character of the clay[1, 3-7] and through the use of different clays and different organic treatments.[8, 9] Among the enhanced properties, fire retardancy is of particular interest in this laboratory.[2-5, 10, 11] The formation of nanocomposites has been accomplished by melt blending, solution blending, and *in situ* polymerization.

In previous work at this laboratory, an ammonium cation containing one styryl group was used, and this material gave a completely exfoliated nanocomposite with styrene[4, 12] and a mixed exfoliated–intercalated nanocomposite with methyl methacrylate.[13] It was suggested that, if polymerization could occur on the cation of the clay, exfoliation was likely. In this study, an ammonium salt containing two styryl groups has been used. This is expected to increase the amount of polymerization that will occur on the clay and should enhance the extent of exfoliation.

EXPERIMENTAL

Materials

The majority of the chemicals used in this study, including styrene, methyl methacrylate, 2,2′-azobisisobutyronitrile, benzoyl peroxide (BPO), vinyl benzyl chloride, *N*-methyloctadecylamine, and initiator removal reagents, were acquired from Aldrich Chemical Co. Pristine sodium montmorillonite was kindly provided by Southern Clay Products, Inc.

Instrumentation

Thermogravimetric analysis (TGA) was performed on an Omnitherm 1000 unit under a flowing nitrogen atmosphere at a scan rate of 10 °C/min from 20 to 600 °C. All TGA results are the averages of a minimum of three determinations; the temperatures are reproducible to ±3 °C, whereas the error bars on the fraction of the nonvolatile material is ±3%. Cone calorimetry was performed with an Atlas Cone 2 instrument according to ASTM E 1354-92 at an incident flux of 35 kW/m^2 or 50 kW/m^2 with a cone-shaped heater. The exhaust flow was set at 24 L/s, and the spark was continuous until the sample ignited. Cone samples were prepared by compression molding of the sample (20–50 g) into square plaques with a heated press. Typical results from cone calorimetry are reproducible to within about ±10%; these uncertainties are based on many runs in which thousands of samples have been combusted.[14] X-ray diffraction (XRD) was performed on a Rigaku Geiger Flex two-circle powder diffractometer; scans were take at 2θ = 0.86–10, a step size of 0.1, and a scan time per step of 10 s. Bright-field transmission electron microscopy (TEM) images of the composites were obtained at 60 kV with a Zeiss 10c electron microscope. The samples were ultramicrotomed with a diamond knife on a Riechert-Jung

Ultra-Cut E microtome at room temperature to give sections approximately 70 nm thick. The sections were transferred from the knife edge to 600 hexagonal mesh Cu grids. The contrast between the layered silicates and the polymer phase was sufficient for imaging, so no heavy metal staining of sections before imaging was required. The mechanical properties were obtained with a Sintech 10 (Systems Integration Technology, Inc.) computerized system for material testing at a crosshead speed of 0.2 in/min. The samples were prepared via injection molding, with an Atlas model CS 183MMX minimax molder, and via stamping from a sheet; the reported values are the averages of five determinations.

Synthesis of *N*-Methyl-*N*,*N*-di(vinylbenzyl)octadecylammonium Chloride

In a 150-mL, round-bottom flask were placed 10.0 g (0.0353 mol) of *N*-methyloctadecylamine, 0.1 g (0.0006 mol) of 4-*tert*-butylcatechol, and 100 mL of tetrahydrofuran (THF). This was stirred until all was completely dissolved at room temperature. A 6.5-g (0.043-mol) portion of vinyl benzyl chloride was added dropwise to the solution at 45 °C over a 2-h period. A 20-mL portion of a 10% aqueous solution of KOH was added dropwise, and the solution was stirred for an additional 2 h. The solvent was evaporated on a rotary evaporator, and the residue was extracted with an ether–water mixture. The ether layer was separated and dried over sodium sulfate. The ether was evaporated, and the residue, together with 25 mL of THF, was transferred to a 50-mL flask. To this solution was added 13 g (0.086 mol) of vinyl benzyl chloride and 0.1 g (0.0006 mol) of 4-*tert*-butyl catechol, and the reaction system was maintained at 50 °C for 2 h. Aliquots were withdrawn and analyzed until all the amine was transformed into the ammonium salt; this typically required 1 h. The reaction mixture was extracted with anhydrous hexane, and the oily product was dried *in vacuo* at room temperature to give 15 g of a pale yellow and viscous product with 97% purity (NMR); the yield was around 79%.

> ^{1}H NMR ($CDCl_3$, δ): 7.53 (dd, *J* = 0.12, 0.03, 8H), 6.71 (dd, *J* = 0.06, 0.04, 2H), 5.83 (d, *J* = 0.06, 2H), 5.37 (d, *J* = 0.04, 2H), 5.16 (d, *J* = 0.04, 2H), 4.91 (d, *J* = 0.04, 2H), 3.18 (m, 2H), 3.13 (s, 3H), 1.90 (br, 2H), 1.08–1.28 (m, 33H), 0.873 (t, *J* = 0.02, 3H).

Preparation of the Ammonium-Modified Clay

A suspension of 10 g of prewashed sodium montmorillonite in 400 mL of distilled water was stirred for 4 h in an Erlenmeyer flask. Then, approximately 400 mL of methanol was added, and stirring was continued overnight. To the stirred and cooled (0–5 °C) clay suspension, a methanol solution of 6.0 g of the previously synthesized organic ammonium salt in 50 mL of methanol was added dropwise. After the solution was stirred overnight at 0–5 °C, the white precipitate was filtered, washed with water at least three times, washed with 80/20 (v/v) methanol/water twice, and washed with water again until no chloride ion could be detected by an acidic aqueous $AgNO_3$ solution. It was then dried in a vacuum oven overnight at room temperature.

Preparation of Polystyrene (PS)–Clay and Poly(methyl methacrylate) (PMMA)–Clay Nanocomposites

In a 400-mL beaker were placed 6 g of organically modified clay, 1 g of BPO as a radical initiator, and 200 g of styrene or methyl methacrylate monomer. This mixture was stirred at room temperature under flowing N_2 gas until it gave a homogeneous suspension, and then it was heated in a water bath at 50 °C until the suspension had hardened somewhat; this was followed by cooling to room temperature. It was then heated at 50 °C for 24 h and at 80 °C for an additional 24 h under an atmosphere of N_2. The unreacted monomer was then removed *in vacuo* (0.1 mmHg) overnight at 100 °C to give the 3% divinyl ammonium modified clay nanocomposite. Other compositions were obtained with the same procedure with different amounts of clay (10, 1.0, and 0.2 g). In some cases, the nanocomposites were melt-blended in a Brabender plasticorder for either 10 or 60 min at a low speed.

Measurement of the Molecular Weight

The nanocomposites were Soxhlet-extracted with toluene as the solvent to obtain the clay-free polymer. The molecular weights were determined by viscosity measurements. The Mark–Houwink constants for PS and PMMA were obtained from the *Polymer Handbook*.[15] Bulk polymerizations of PS and PMMA were carried out by the same procedure in the absence of clay. The viscosity-average molecular weight of the extracted polymers and the controls was 60,000 ± 10,000.

RESULTS AND DISCUSSION

In previous work at this laboratory, an ammonium cation containing two methyl groups, one hexadecyl group, and one styryl group was used.[4, 12] When the bulk polymerization of styrene was performed with this cation to render the clay sufficiently organophilic to enable the formation of a nanocomposite, approximately 5% of the styrene was found to polymerize onto the cation, and the resulting nanocomposite was best described as completely exfoliated. In the case of methyl methacrylate nanocomposites with this cation, a mixed exfoliated–intercalated material was obtained. On the basis of this work, we believe that exfoliation is likely if polymerization occurs through the cation on the clay. Accordingly, a cation was produced containing two styryl groups, a methyl chain, and a hexadecyl chain; this cation, and the clay treated with it, are called divinyl, and the nanocomposites are divinyl polystyrene (DPS) and divinyl poly(methyl methacrylate) (DPMMA). The structure of this cation is shown in **Figure 1**. The expectation is that exfoliation will be more complete than that seen for the cation with only one styryl group.

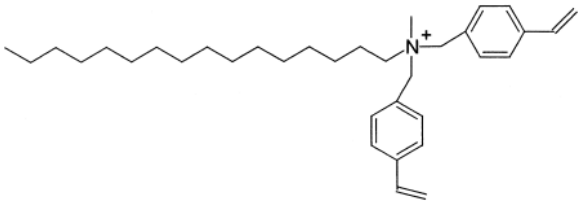

Figure 1 Structure of the cation used in this study.

To determine how much, if any, styrene was attached to the clay, we extracted the nanocomposites with toluene. The insoluble material consisted of clay, along with any polymer still attached. The results are shown in **Table 1**. For PS, the recovered material was approximately twice the amount of clay initially present in the nanocomposite, and it was even larger for methyl methacrylate. This indicates that polymerization occurred onto the cation bound to the clay. At the smallest amount of clay used, 0.1%, no material was recovered. It is likely that this small amount of clay remained suspended in the extraction solvent and could not be recovered.

Table 1. Recovery of the Clay and Polymer Attached to the Clay from PS and PMMA Nanocomposites

Nanocomposite	Calculated Clay Content (%)	Clay Recovered (%)
5% DPS	5.9	14.0
3% DPS	3.2	5.7
0.5% DPS	0.6	0.9
0.1% DPS	0.1	—
5% DPMMA	5.5	18.9
3% DPMMA	3.3	7.9
0.5% DPMMA	0.5	0.5
0.1% DPMMA	0.1	—

XRD Measurements

The *d*-spacing observed for the sodium clay was 1.2 nm, and this increased to 2.3 nm when the divinyl cation was attached to the clay. The XRD results for PMMA nanocomposites are shown in **Figure 2**, and those for styrene are shown in **Figure 3**. For PMMA, a peak near 2θ = 4 can clearly be seen for the clay, whereas for the nanocomposites, a small peak near 2θ = 2 is evident at high clay contents but not at lower clay contents. Similar results were observed for the PS system.

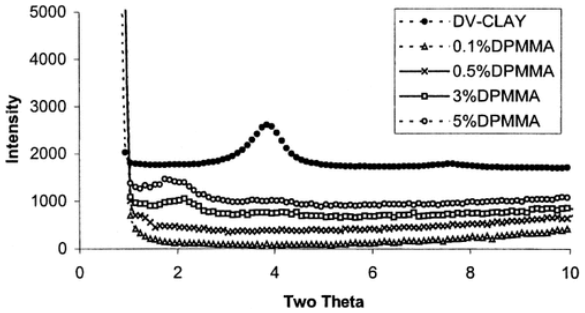

Figure 2 XRD curves of PMMA/divinyl modified clay nanocomposites.

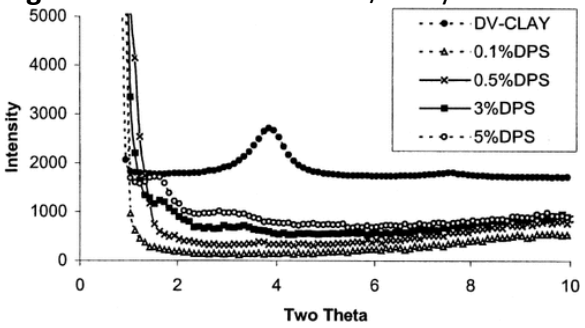

Figure 3 XRD curves of PS/divinyl modified clay nanocomposites.

TEM Results

TEM images at low and high magnifications are shown in **Figure 4** for PMMA and in **Figure 5** for PS. It is obvious from the low-magnification images that the clay was well dispersed throughout the polymer and that a nanocomposite was indeed formed. The higher magnification images show that these were exfoliated materials, as would be expected for PS because a completely exfoliated material was produced from the monostyryl cation. These materials were subjected to melt blending in a Brabender mixer, and TEM images were again recorded. These results are shown in **Figure 6** for PMMA and in **Figure 7** for PS. It is clear from the low-magnification images that the dispersion was even better after melt blending. This may suggest that melt blending of *in situ* polymerized nanocomposites may improve the dispersion of the clay.

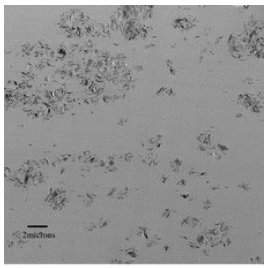

(a)

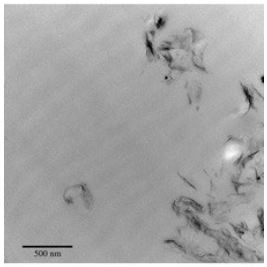

(b)

Figure 4 TEM images of the PMMA nanocomposite with divinyl-substituted clay at (a) low magnification and (b) medium magnification.

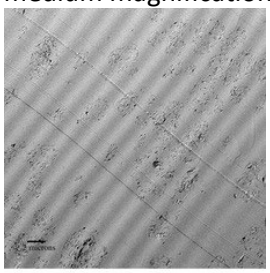

(a)

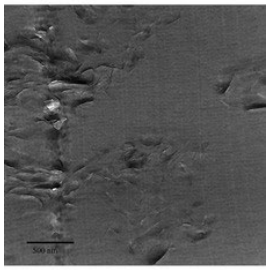

(b)

Figure 5 TEM images of the PS nanocomposite with divinyl-substituted clay at (a) low magnification and (b) medium magnification.

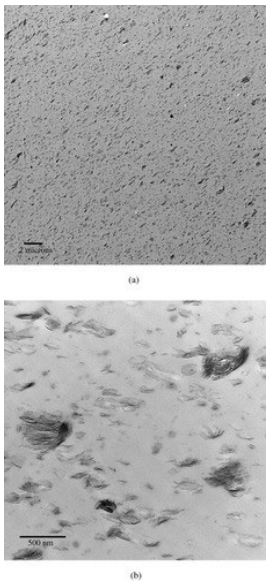

Figure 6 TEM images of the PMMA nanocomposite with divinyl-substituted clay at (a) low magnification and (b) medium magnification after melt blending.

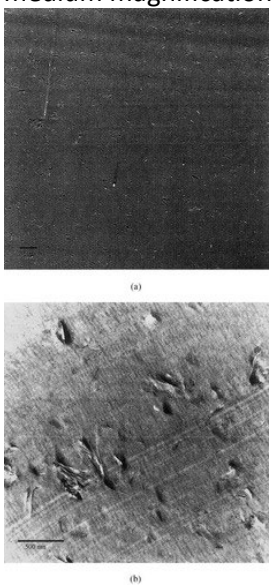

Figure 7 TEM images of the PS nanocomposite with divinyl-substituted clay at (a) low magnification and (b) medium magnification aftermelt blending.

Mechanical Properties of the Nanocomposites

The mechanical properties of the nanocomposites are shown in **Table 2**. For the PS nanocomposites, there was a small increase in the elongation as the amount of clay increased, whereas the tensile strength decreased and Young's modulus increased. For PMMA, there was a definite increase in both the tensile strength and Young's modulus. Previous literature[1] suggests that Young's modulus is higher for exfoliated nanocomposites than for virgin polymer and intercalated nanocomposites. Noh and Lee[16] reported both stress and strain for PS nanocomposites prepared by the emulsion polymerization of styrene with a sodium clay. The stress at maximum load decreased for the nanocomposite relative to the virgin polymer, and Young's modulus increased; their values are comparable to those obtained in this study. For PMMA, Lee and Jang[17] showed that both the stress at maximum load and Young's modulus increased for the nanocomposites prepared by emulsion polymerization with the sodium clay in comparison to the virgin polymer. They prepared materials containing a much higher

clay content, and their reported Young's modulus was substantially higher than observed in this work. It has been suggested that the modulus increases as the amount of exfoliation increases.[1] In previous work from these laboratories,[18] we have shown that there is no apparent correlation between the type of nanocomposite, exfoliated or intercalated, and the tensile strength or Young's modulus for PS and PMMA nanocomposites. These mechanical properties have also been evaluated after melt blending for either 10 min or 1 h at 200 °C, and it was found that melt blending has essentially no effect on the mechanical properties; that is, even though the dispersion of clay appears to be better by TEM after melt blending, this does not affect the mechanical properties.

Table 2. Mechanical Properties of the PS and PMMA Nanocomposites

Nanocomposite	Elongation (%)	Modulus (GPa)	Tensile Strength (MPa)
PS	1.2	1.31	18.04
0.1% DPS	1.3	1.28	9.28
0.5% DPS	1.2	1.46	14.57
3% DPS	1.4	1.57	18.22
5% DPS	1.7	1.24	10.38
PMMA	3.8	0.92	18.14
0.1% DPMMA	5.5	1.28	38.24
0.5% DPMMA	2.6	1.15	24.39
3% DPMMA	3.0	1.09	21.46
5% DPMMA	3.1	1.42	30.53

TGA Characterization of the Nanocomposites

The thermal stability in nitrogen of both PS–clay and PMMA–clay nanocomposites was enhanced relative to that of virgin polymers, as shown in **Figures 8** and **9**. Typically, the onset temperature of the degradation increased by about 50 °C for PS–clay nanocomposites and between 50 and 100 °C for PMMA–clay nanocomposites. If one looks closely at the TGA curve for the PMMA–clay nanocomposites, a second step can be seen in the degradation. Kashiwagi et al.[19] described three steps in the degradation of radically polymerized PMMA, and these are attributed to cleaving head-to-head linkages, chain end unsaturation initiating depolymerization, and random scission. These are usually only observed at very slow scan speeds. It is possible that the steps seen in the TGA curve may be attributable to these processes, and in the following, we offer an explanation in these terms. In these curves, the loss of head-to-head linkages is not resolved from that due to chain end unsaturation, but at higher clay contents, two steps are evident, and one may also see this at 0.5% clay in comparison to curves for higher amounts of clay. The additional step was also seen when the clay with only a single vinyl group was used. It is apparent that the presence of the clay stabilizes both steps of the degradation.[13]

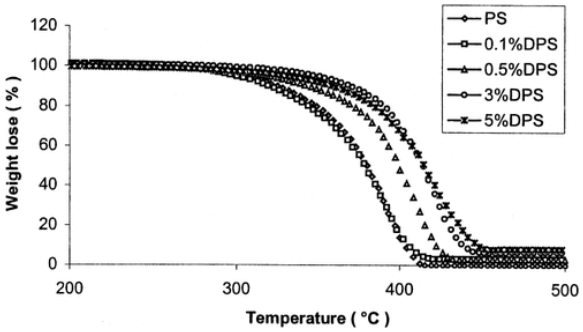

Figure 8 TGA curves for PS and its nanocomposites.

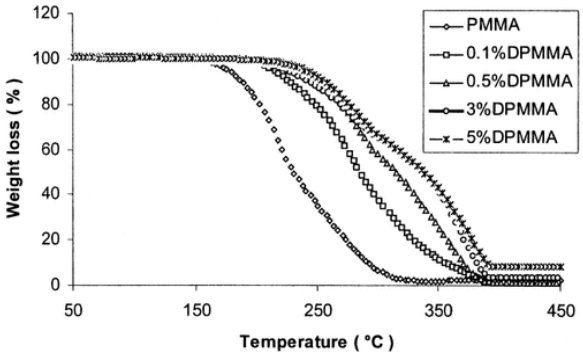

Figure 9 TGA curves for PMMA and its nanocomposites.

TGA was also performed on the insoluble material extracted from these nanocomposites. This consisted of the clay along with the polymer polymerized onto the clay. The curves for the PS samples show that the material recovered from the 0.5% nanocomposite had the latest onset of degradation and the greatest fraction of material that was nonvolatile at 600 °C. This was expected because the small amount of clay present in the nanocomposite meant the smallest fraction of organic material and, therefore, the smallest amount of material capable of degradation and the smallest amount of monomer onto which polymerization could occur. The 3% nanocomposite underwent the easiest degradation, whereas the 5% nanocomposite was the most thermally stable. The fraction of material that was nonvolatile at 600 °C was 32% for the 0.5% nanocomposite, 29% for the 3% nanocomposite, and 21% for the 5% nanocomposite. The clay itself gave an 80% residue at 600 °C, and so putting together the data from the amounts of the insoluble material and these residues, one can calculate that 0.5% of the polymer was incorporated into the 0.5% nanocomposite, 3.6% was incorporated into the 3% nanocomposite, and 10.4% was incorporated into the 5% nanocomposite; the TGA curves for these materials are shown in **Figure 10**.

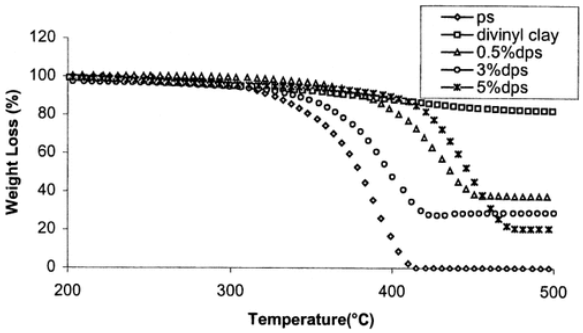

Figure 10 TGA curves for the insoluble portion of PS nanocomposites.

Similar results were obtained for the insoluble portion of the PMMA nanocomposite. At least two steps can be seen in the thermal degradation of the polymer portion for both the 3 and 5%, but not 0.5%, nanocomposites. Once again, the greatest organic residue was seen for the 0.5% nanocomposite (32%), with lesser amounts for the others (3% nanocomposite, 29% residue; 5% nanocomposite, 23% residue), and the same explanation holds as for PS. This data enable us to calculate the amount of polymerization occurring onto the cation: 0.3% for the 0.5% nanocomposite, 5.1% for the 3% nanocomposite, and 13.4% for the 5% nanocomposite. These numbers are very similar to what was observed for the PS nanocomposites, and they suggest that both monomers are able to react to about the same extent; this implies that the important step is the encounter between the cation and the propagating chain. The TGA curves are shown in **Figure 11**.

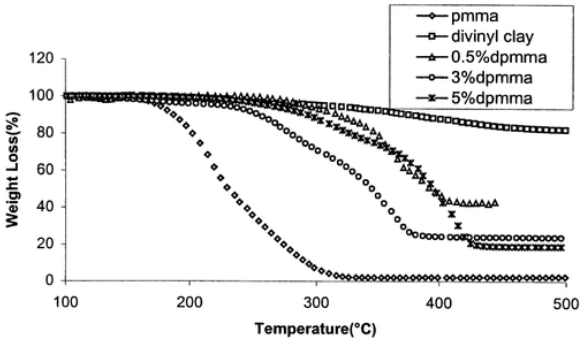

Figure 11 TGA curves for the insoluble portion of PMMA nanocomposites.

Fire Performance of the Nanocomposites

The fire properties of the nanocomposites were assessed by cone calorimetry. Ideally, one would like to observe a decrease in the rate of heat release, an increase in the time to the peak heat release rate and time to ignition, a reduced mass loss rate, and a decrease in the smoke evolution (specific extinction area). The results for PS are shown in **Table 3**, and a plot of the heat release rates is shown in **Figure 12**; the data for PMMA are in **Table 4** and **Figure 13**. For both polymers, the time to ignition and the time to the peak heat release rate (PHRR) stayed quite constant over the entire range, from 0 to 5% clay. The mass loss rate and the peak heat release rate decreased as the amount of clay increased, and the mass loss at the time at which the virgin polymer was essentially completely burned (160 s for PS and 190 s for PMMA) also decreased.

Table 3. Cone Calorimetry Data for PS and Its Nanocomposites at 35 kW/m^2

Composition	**PS**	**DPS0.1**	**DPS0.5**	**DPS3**	**DPS5**
Time to ignition (s)	51 ± 3	49 ± 3	48 ± 3	53 ± 2	45 ± 5
PHRR (kW/m^2)	1381 ± 18	1292 ± 101	1263 ± 55	867 ± 82	741 ± 28
Time to PHRR (s)	67 ± 6	60 ± 1	67 ± 3	68 ± 4	73 ± 4
Time to burnout (s)	189 ± 7	192 ± 3	195 ± 7	213 ± 15	262 ± 4
Energy released through 160 s, (MJ/m^2)	92 ± 7	88 ± 2	95 ± 1	90 ± 4	90 ± 2
Average heat released (kW/m^2)	487 ± 42	462 ± 15	488 ± 24	427 ± 23	360 ± 10
Total heat released (MJ/m^2)	92 ± 7	88 ± 2	95 ± 1	91 ± 4	94 ± 4
Average mass loss rate (g/sm^2)	13.9 ± 1.4	13.1 ± 0.3	12.9 ± 0.5	11.1 ± 1.4	9.5 ± 0.4
Mass loss at 160 s (%)	76 ± 10	72 ± 2	63 ± 3	58 ± 6	47 ± 6
Average specific extinction area (m^2/kg)	1218 ± 73	1418 ± 172	1564 ± 78	1653 ± 124	1962 ± 127

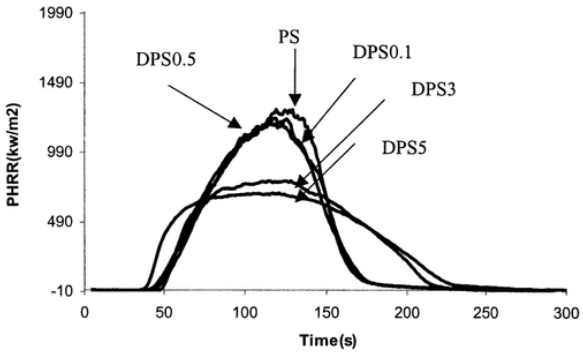

Figure 12 Heat release rate of PS/divinyl modified clay nanocomposites.

Table 4. Cone Calorimetry Data for PMMA and Its Nanocomposites at 35 kW/m^2

Composition	PMMA	DPMMA0.1	DPMMA0.5	DPMMA3	DPMMA5
Time to ignition (s)	18 ± 3	21 ± 3	19 ± 4	19 ± 3	26 ± 4
PHRR (kW/m^2)	842 ± 5	870 ± 45	862 ± 45	628 ± 6	585 ± 97
Time to PHRR (s)	83 ± 3	95 ± 5	87 ± 8	90 ± 7	85 ± 7
Time to burnout (s)	215 ± 5	217 ± 25	206 ± 27	228 ± 15	300 ± 6
Energy released through 190 s (MJ/m^2)	85 ± 4	90 ± 5	87 ± 7	82 ± 3	84 ± 1
Average heat released (kW/m^2)	398 ± 12	417 ± 32	425 ± 26	367 ± 15	309 ± 37
Total heat released (MJ/m^2)	86 ± 5	90 ± 5	87 ± 7	83 ± 4	88 ± 4
Average mass loss rate (g/sm^2)	11.2 ± 0.4	13.0 ± 0.7	13.5 ± 0.4	11.9 ± 0.6	9.8 ± 0.7
Mass loss at 190 s (%)	68 ± 2	74 ± 7	79 ± 5	69 ± 2	54 ± 2
Average specific extinction area (m^2/kg)	24 ± 5	45 ± 4	62 ± 5	69 ± 7	123 ± 6

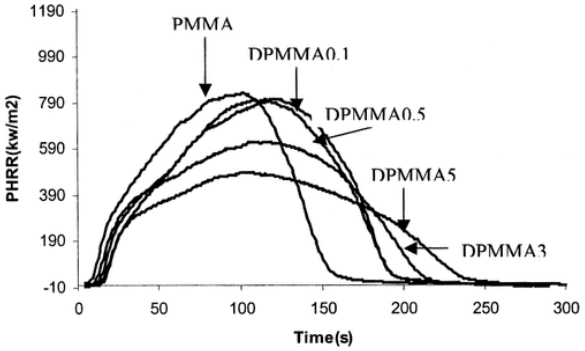

Figure 13 Heat release rate of PMMA/divinyl modified clay nanocomposites.

Cone calorimetry was also performed on the nanocomposites after melt blending, and these results are shown in **Tables 5** and **6**. There was only one obvious change due to melt blending: the time to ignition was less for PS nanocomposites and was increased for PMMA nanocomposites. All other cone parameters appeared to be unchanged by melt blending.

Table 5. Cone Calorimetry Data for 3% Divinyl Modified Clay PS and Its Nanocomposites before and after Melt Blending

Composition	PS	PS (200 °C, 10 min)	DPS3	DPS3 (200 °C, 10 min)	DPS3 (200 °C, 1 h)
Time to ignition (s)	51 ± 3	54 ± 4	53 ± 2	42 ± 1	43 ± 4
PHRR (kW/m^2)	1381 ± 18	1208 ± 8	867 ± 82	842 ± 24	768 ± 18
Time to PHRR (s)	67 ± 6	66 ± 8	68 ± 4	74 ± 5	69 ± 5
Time to burnout (s)	189 ± 7	179 ± 9	213 ± 15	202 ± 4	218 ± 2
Energy released through 160 s (MJ/m^2)	92 ± 7	103 ± 7	90 ± 4	89 ± 2	95 ± 2 (160s)
Average heat released (kW/m^2)	487 ± 42	575 ± 13	427 ± 23	440 ± 15	442 ± 8
Total heat released (MJ/m^2)	92 ± 7	103 ± 7	91 ± 4	89 ± 1	96 ± 2
Average mass loss rate (g/s)	13.9 ± 1.4	16.0 ± 1.0	11.1 ± 1.4	13.9 ± 0.4	14.1 ± 1.3
Mass loss at 190 s (%)	76 ± 10	89 ± 5	58 ± 6	78 ± 3	75 ± 6
Average specific extinction area (m^2/kg)	1218 ± 73	1207 ± 2	1653 ± 124	1289 ± 21	1463 ± 155

Table 6. Cone Calorimetry Data for 3% Divinyl Modified Clay PMMA and Its Nanocomposites before and after Melt Blending

Composition	**PMMA**	**PMMA (195 °C, 10 min)**	**DPMMA3**	**DPMMA3 (195 °C, 10 min)**	**DPMMA3 (195 °C, 1 h)**
Time to ignition (s)	18 ± 3	14 ± 1	19 ± 3	29 ± 1	35 ± 2
PHRR (kW/m^2)	842 ± 5	836 ± 8	628 ± 6	672 ± 10	684 ± 18
Time to PHRR (s)	83 ± 3	80 ± 6	90 ± 7	59 ± 2	57 ± 5
Time to burnout (s)	215 ± 5	217 ± 1	228 ± 15	197 ± 16	230 ± 12
Energy released through 190 s (MJ/m^2)	85 ± 4	85 ± 1	82 ± 3	78 ± 9	92 ± 1
Average heat released (kW/m^2)	398 ± 12	393 ± 1	367 ± 15	356 ± 17	400 ± 25
Total heat released (MJ/m^2)	86 ± 5	85 ± 1	83 ± 4	78 ± 8	92 ± 1
Average mass loss rate (g/s)	11.2 ± 0.4	14.3 ± 0.1	11.9 ± 0.6	13.8 ± 0.2	13.9 ± 0.9
Mass loss at 190 s (%)	68 ± 2	87 ± 1	69 ± 2	86 ± 1	82 ± 4
Average specific extinction area (m^2/kg)	24 ± 5	12 ± 3	69 ± 7	36 ± 3	69 ± 7

CONCLUSIONS

When PS and PMMA are bulk-polymerized in the presence of a clay that contains distyryl quaternary ammonium monomers, exfoliated nanocomposites result. The extent of dispersion of the clay within the polymer can be increased by melt blending, but this appears to have no effect on the mechanical properties or flammability characteristics, except that the time to ignition is reduced for PS nanocomposites and increased for PMMA systems.

Acknowledgements

This work was performed under the sponsorship of the U.S. Department of Commerce through the National Institute of Standards and Technology (70NANB6D0119). The authors thank Peggy Miller (University of Texas Health Center at San Antonio) and Ryan Dennis (Southern Clay Products) for obtaining the transmission electron micrographs.

REFERENCES AND NOTES

1 Alexandre, M.; Dubois, P. *Mater Sci Eng R* 2000, **28**, 1– 6.
2 Kojima, Y.; Usuki, A.; Kawasumi, M.; Okada, A.; Fukushima, Y.; Kurauchi, T.; Kamigaito, O. *J Mater Res* 1993, **8**, 1185– 1189.
3 Zhu, J.; Wilkie, C. A. *Polym Int* 2000, **49**, 1158– 1163.
4 Zhu, J.; Morgan, A. B.; Lamelas, F. L.; Wilkie, C. A. *Chem Mater* 2001, **13**, 3774– 3780.
5 Ruitz-Hitzky, E.; Casal, B. *Nature* 1978, **276**, 596– 597.
6 Gilman, J. W.; Kashiwagi, T. A.; Morgan, B.; Harris; R. H., Jr.; Brassell, L.; Award, W. H.; Davis, R. D.; Chyall, L.; Sutto, T.; Trulove, P. C.; Delong, H. Proc Add 2001.
7 Yao, H.; Zhu, J.; Morgan, A. B.; Wilkie, C. A. *Polym Eng Sci* 2002, **42**, 1808– 1814.
8 Kornmann, X.; Berglund, L. A.; Sterte, J. *Polym Eng Sci* 1998, **38**, 1351– 1358.
9 Wang, Z.; Pinnavaia, T. *J Polym Mater Sci Eng* 2000, **82**, 274.
10 Gilman, J. W.; Kashiwagi, T.; Giannelis, E. P.; Manias, E.; Lomakin, S.; Litchtenham, J. D.; Jones, P. In *Fire Retardancy of Polymers: The Use of Intumescence*; M. Le Bras; G. Camino; S. Bourbigot; R. Delobel, Eds.; Royal Society of Chemistry: London, 1998; pp 201– 221.
11 Shu, Z.; Chen, G.; Qi, Z. *Suliao Gongye* 2000, **28**, 24– 26.

12 Zhu, J.; Uhl, F. M.; Morgan, A. B.; Wilkie, C. A. *Chem Mater* 2001, **13**, 4649– 4654.
13 Zhu, J.; Start, P.; Mauritz, K. A.; Wilkie, C. A. *Polym Degrad Stab* 2002, **77**, 253– 258.
14 Gilman, J. W.; Kashiwagi, T.; Nyden, M.; Brown, J. E. T.; Jackson, C. L.; Lomakin, S.; Giannelis, E. P.; Manias, E. In *Chemistry and Technology of Polymer Additives*; S. Al-Malaika; A. Golovoy; C. A. Wilkie, Eds.; Blackwell Scientific: Oxford, 1999; pp 249– 265.
15 Kurata, M.; Tsunashima, Y. In *Polymer Handbook*, 4th ed.; J. Brandrup; E. H. Immergut; E. A. Grulke, Eds.; Wiley: New York, 1999; Chapter 7, pp 1– 83.
16 Noh, M. W.; Lee, D. C. *Polym Bull (Berlin)* 1999, **42**, 619– 626.
17 Lee, D. C.; Jang, L. W. *J Appl Polym Sci* 1996, **61**, 1117– 1122.
18 Wang, D.; Zhu, J.; Yao, Q.; Wilkie, C. A. *Chem Mater* 2002, **14**, 3827.
19 Kashiwagi, T.; Inaba, A.; Brown, J. E.; Hatada, K.; Kitayama, T.; Masuda, E. *Macromolecules* 1986, **19**, 2160– 2168.